GENERATION OF HIGH-FREQUENCY P AND S WAVE ENERGY BY ROCK FRACTURE DURING A BURIED EXPLOSION: ITS EFFECT ON P/S DISCRIMINANTS AT LOW MAGNITUDE

Charles Sammis

University of Southern California

Sponsored by Defense Threat Reduction Agency

Contract No. DTRA01-01-C-0086

ABSTRACT

The growth of pre-existing fractures is an important physical process that contributes to the generation of high-frequency seismic waves by explosions. Characterized as damage, this crack growth affects the seismic source in two important ways. First, increased damage weakens the rock by lowering its elastic modulus. Second, the growing fractures act as secondary sources of seismic energy. This secondary energy may further weaken crushed rock in the source region by "acoustic fluidization," and it may make a significant contribution to the far-field radiation. Secondary seismic radiation is investigated here using an equivalent elastic method to approximate the stress field surrounding an underground explosion and a micro-mechanical damage mechanics model to calculate the associated increase in damage. Because our damage mechanics calculates the nucleation and growth of individual fractures, a seismic moment tensor can be found for each. Integration over all such growing cracks yields secondary elastic waves that radiate into the far field. While the contribution from an individual crack is small, the combined effect of many cracks in a large region of increased damage can produce primary waves comparable in amplitude to those generated directly by the explosion. Any asymmetry in the growth of damage is very effective in generating S waves. Sources of asymmetry investigated here include a pre-existing tectonic shear stress or a preferred orientation of initial cracks. The effect of different lithologies is primarily reflected in the initial damage and size of the initial flaws. The amount of new damage is controlled primarily by the initial damage, while the size of the zone of new damage is controlled primarily by the size of the initial flaws.

OBJECTIVE

Introduction

Several different processes occur in the rock near a tamped underground explosion, as illustrated in Figure 1 (see, e.g., Rodean, 1971). The explosion is initially contained within a cavity of radius r_c, which has been excavated from the surrounding rock. At the time of detonation a hot pressurized gas is created within the cavity, which causes it to expand. Some of the surrounding rock may be vaporized and added to the cavity gas at this time. The sudden expansion of the cavity generates a shock wave that propagates outward causing major damage to the surrounding rock and producing the series of regimes summarized in Figure 1. Rock first flows plastically; then is stressed beyond its brittle failure limit and becomes granulated; then is stressed to the point where radial cracks grow but failure is not reached; then deforms anelastically where pre-existing cracks slide but do not grow; and finally deforms elastically. These regimes reflect the decrease in energy density in the shock with distance from the explosion caused partly by spherical spreading and partly by the fact that energy is being used to fracture and deform the rock. The shock wave gradually decays into an inelastic wave involving non-linear motions, which further decays with distance until a radius is reached where the motions are small enough to be described by the ordinary elastodynamic equations of linear elasticity. Beyond this elastic radius, r_e, the disturbance caused by the explosion can be modeled as linear elastic waves that propagate throughout the rest of the earth.

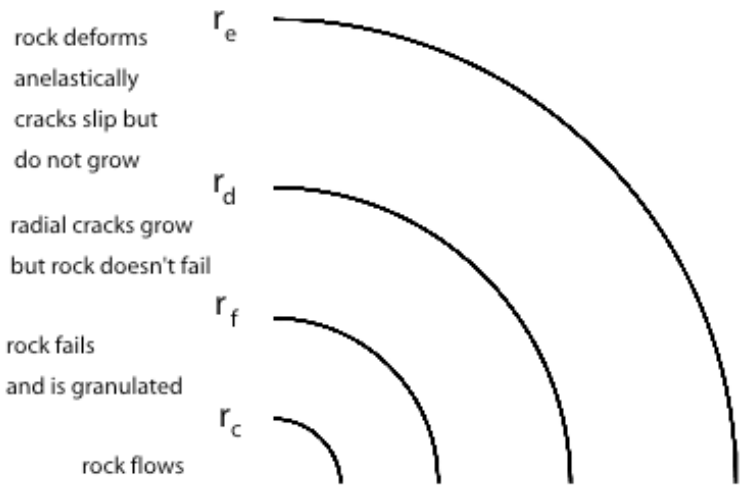

Figure 1. Schematic diagram of the region surrounding a contained explosion in rock: r_c is the cavity radius, r_f is the radius to which failure occurs, r_d is the radius to which new damage is created, and r_e is the elastic radius beyond which waves can be approximated as elastic.

These processes that occur around an explosion can have strong effects on the elastic waves that are radiated beyond the elastic radius r_e. In this report we concentrate on the growth of pre-existing cracks that can affect the radiated elastic waves in at least three different ways. First, intense cracking will significantly lower the bulk modulus and shear modulus near the source (O'Connell and Budianski, 1974; Rimer *et al*. 1998). Second, it has been speculated that when cracking extends into the failure regime, acoustic fluidization can lower the basic strength of the rock (Sammis, 1998). Third, motions on the cracks serve as secondary sources of elastic waves that can contribute to the net seismic radiation field. The primary objective of the work reported here is to provide a quantitative assessment of this third phenomenon. The intent is to determine how these secondary sources modify the P and S waves generated by the explosion and radiated to the far field.

We approach this problem by using the formulation of Ashby and Sammis (1990) to model the nucleation and growth of cracks in the source region, which is here referred to as damage. Calculation of this damage requires knowledge of the stress field in the region surrounding the source, which is approximated in this study by the equivalent elastic method. The micro-mechanical model of damage provides the parameters necessary to represent each crack as a seismic moment tensor that is then used to calculate the elastic waves radiated by the damage.

Finally, we consider the cumulative effect of all the cracks in the damage zone in order to estimate the contribution of damage to P and S waves in the far field.

RESEARCH ACCOMPLISHED

Damage Mechanics

The concept of damage used here is that developed by Ashby and Sammis (1990). In that paper, the conditions under which an initial crack can nucleate additional cracking are derived. Only the basic equations needed to calculate the increase in damage at the shock front will be repeated here. In 3-D, the initial damage is defined as

$$D_0 = \tfrac{4}{3}\pi\left(a\cos\chi\right)^3 N_V\,, \tag{1}$$

where a is the radius of penny-shaped cracks, χ is angle describing the orientation of the cracks (see Figure. 2) and N_V is the number of cracks per unit volume. In response to loading, wing cracks of length l grow at opposite edges of the initial crack thereby increasing the damage to

$$D = \tfrac{4}{3}\pi\left(l + a\cos\chi\right)^3 N_V\,. \tag{2}$$

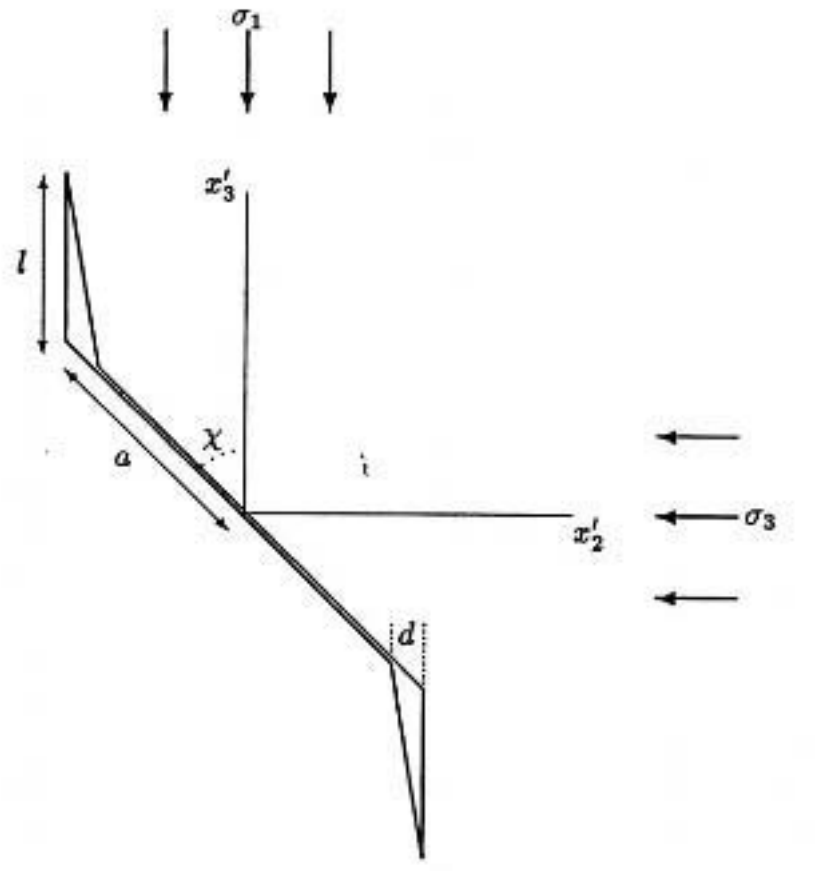

Figure 2. Geometry of a penny-shaped crack of radius *a,* which is extended by wing cracks of length *l*.

The value of l is determined by letting the wing cracks grow until the stress intensity factor at the tip decreases to the fracture toughness of the medium. The equation that must be solved to determine the final amount of damage is (Ashby and Sammis, 1990)

$$S_1 = -\frac{C_2\left(\left(\frac{D}{D_0}\right)^{1/3} - 1 + \frac{\beta}{\cos\chi}\right)^{2/3} - S_3\left[C_1\left(1 + \left(\frac{C_3 D_0^{2/3}}{1-D^{2/3}}\right)\left(\left(\frac{D}{D_0}\right)^{1/3} - 1\right)^2\right) + C_4\left(\left(\frac{D}{D_0}\right)^{1/3} - 1\right)^2\right]}{1 + \frac{C_3 D_0^{2/3}}{1-D^{2/3}}\left(\left(\frac{D}{D_0}\right)^{1/3} - 1\right)^2} \tag{3}$$

Here S_1 and S_3 are the maximum and minimum normalized principal compressive stresses given by

$$S_1 = \frac{\sigma_1}{K_{Ic}/\sqrt{\pi a}}, \qquad S_3 = \frac{\sigma_3}{K_{Ic}/\sqrt{\pi a}} \tag{4}$$

and K_{Ic} is the critical stress intensity for mode I cracks, a material property. The constants in (3) are

$$\begin{aligned} C_1 &= \frac{\left(1+\mu^2\right)^{1/2} + \mu}{\left(1+\mu^2\right)^{1/2} - \mu} \\ C_2 &= \pi(\cos\chi)^{3/2}\sqrt{3/\beta}\,\frac{1}{\left(1+\mu^2\right)^{1/2} - \mu} \\ C_3 &= 2 \\ C_4 &= 2\pi(\cos\chi)^2\sqrt{3/\beta}\,\frac{1}{\left(1+\mu^2\right)^{1/2} - \mu} \end{aligned} \tag{5}$$

In these last equations, μ is the coefficient of static friction and β is a correction factor for the effective length of the crack, typically 0.45 introduced by Ashby and Sammis (1990) to bring their approximate analytical model into agreement with numerical simulations in the limit of small *l*. Also, χ is assumed here to be 45°.

Given the initial damage D_0 and the principal stresses σ_1 and σ_3, equation (3) can be used to calculate the equilibrium state of damage. This is a cubic equation in the damage, which we solve numerically. There are three possible outcomes. At low stresses, wing cracks do not nucleate and we get no real solutions. At intermediate stresses we calculate a value of $D>D_0$ until a maximum is reached above which we again get no real solutions. Ashby and Sammis (1990) interpret this maximum as failure since, for additional loading, damage increases at decreasing stress, an unstable condition leading to shear localization. We do not attempt to model this post-failure regime beyond identifying it as the granulated region described in the introduction, and as a possible site for further weakening by acoustic fluidization.

Stress Field Surrounding an Explosion – The Effective Elastic Medium

In order to model the increase in damage, we require the principal stresses generated by the explosion as a function of distance and time. This is made difficult by the existence of the nonlinear processes between the cavity radius and the effective elastic radius, beyond which the assumptions of ordinary linear elasticity are valid. Sophisticated computer codes have been developed which include hydrodynamic effects, shock waves, and nonlinear equations of state (see, for example, Rodean, 1971; King *et al*., 1989; Glenn, 1993; Glenn and Goldstein, 1994, for discussion and further references). We use here an approximate method to calculate the stresses surrounding an explosion that is based on the equivalent elastic method developed by earthquake engineers to model the nonlinear behavior of soils that that occurs during strong ground motion. The central idea is to make the material properties a function of the stress in the outward propagating pressure pulse and then to adjust these material properties in an iterative process until the appropriate values are present at all distances from the source. In effect, the nonlinear stress-strain behavior is approximated by a series of linear relationships that change with the level of stress. The present

formulation, described by Johnson (1993), relates density and bulk elastic properties to the peak pressure and shear and anelastic properties to the maximum shear strain.

The details of this model are published in Johnson and Sammis (2001) and will not be repeated here. In that paper we modeled the 1 kt chemical explosion detonated in September 1993 as part of the Non-Proliferation Experiment (NPE) (see Denny, 1994). The results of this simulation and attendant damage calculations are summarized in the next section.

Simulation of the NPE Explosion

The first objective in modeling the 1993 NPE event was to check the ability of the equivalent elastic method to simulate the stress field around and explosion. As illustrated in Figure 3 the model gives reasonable values for the peak velocity as a function of distance out to about one kilometer beyond which the model predicts slightly higher velocities than those observed. The calculated waveforms (Figure 4) were also comparable to those observed except for a bit of excessive reverberation.

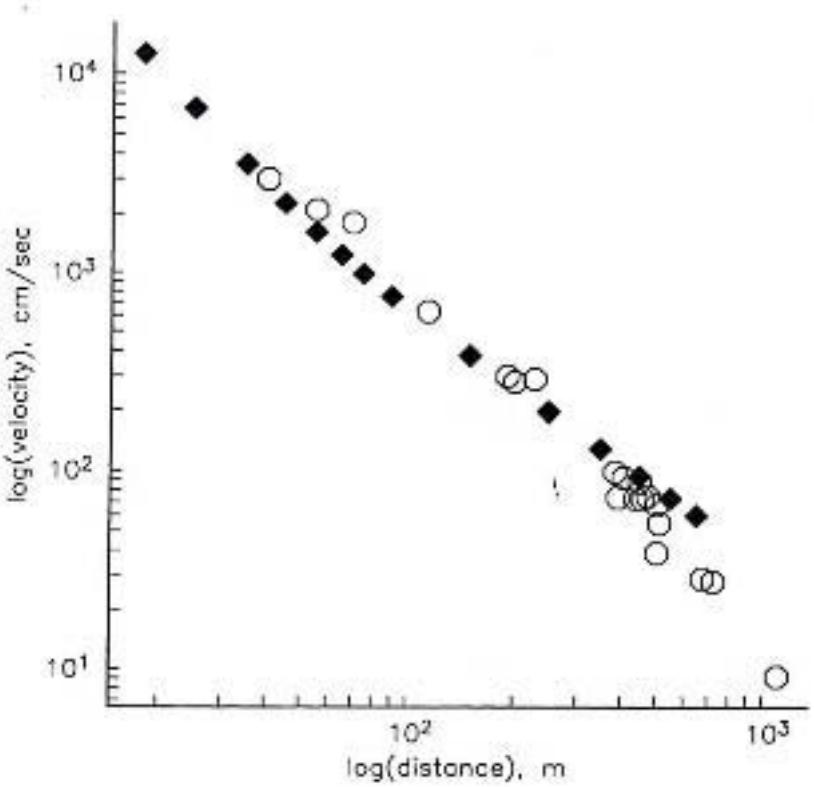

Figure 3. Measured and calculated peak velocities for the NPE explosion. The open symbols are observations taken from Smith (1994) and Olsen and Peratt (1994), while the filled symbols were calculated with the equivalent elastic method (from Johnson and Sammis, 2001).

Having established that the equivalent elastic method gives a good approximation to the observed motions close to the NPE explosion, we now asked whether stresses were sufficiently high to produce an increase in damage. As illustrated in Figure 5, the shock front does indeed produce an increase in damage at a distance of 35 m. Note that the damage does not increase during peak load, but during unloading when the tangential (hoop) stress decreases more rapidly than the radial stress.

Finally, we asked whether the seismic radiation generated by the increase in crack damage makes a significant contribution to the seismic signal in the far field. In order to do this we derived a moment tensor representation of the damage and then calculated the radiated elastic waves using a Green function approach.

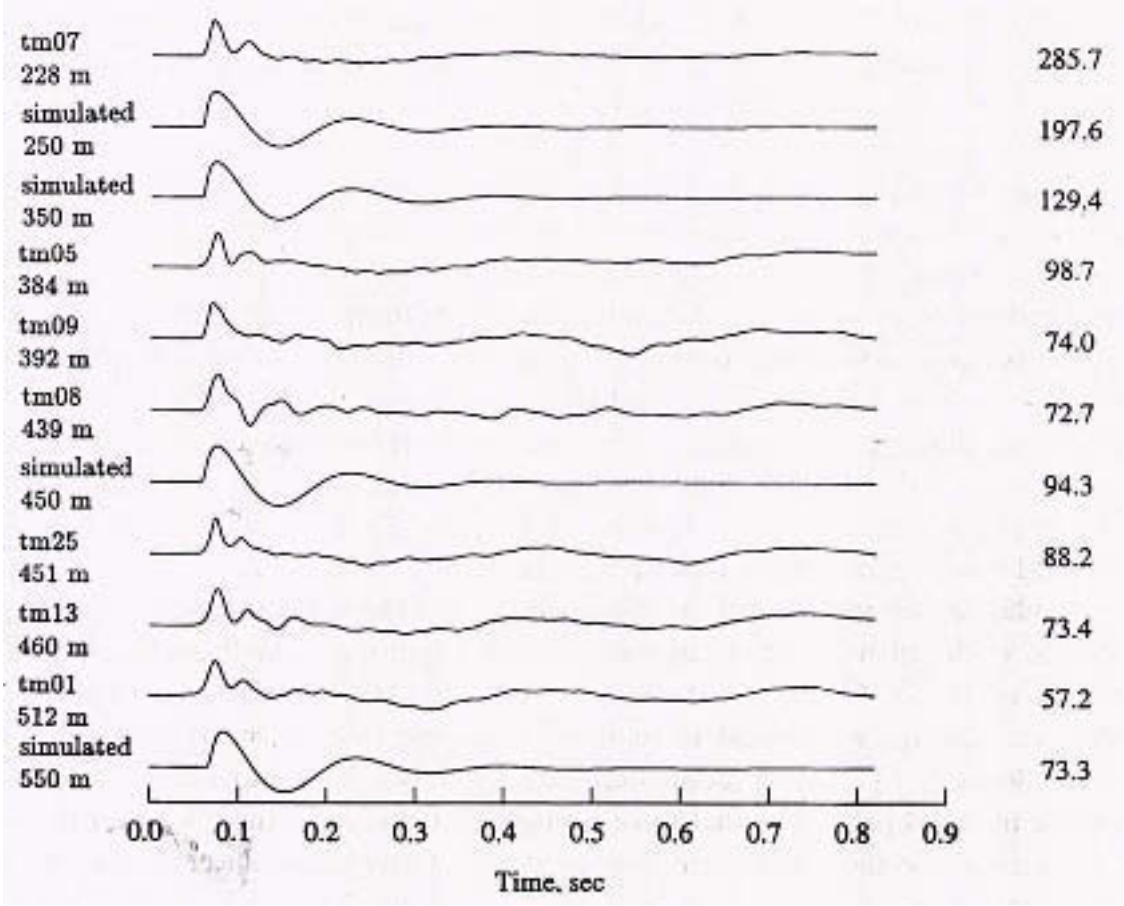

Figure 4. Comparison between measured and calculated waveforms for the NPE explosion. The traces labeled with tm are the radial velocities measured by Olsen and Peratt (1994) at the radial distances shown. The traces labeled with simulated are the radial velocities calculated with the equivalent elastic method at the radial distances shown. The numbers on the right are maximum velocities on the traces in units of cm/sec (from Johnson and Sammis, 2001).

The damage of Ashby and Sammis (1990) is modeled as an initial crack that is extended by wing cracks. Johnson and Sammis (2001) represented this as the combination of two separate source moment tensors: shear dislocation on the initial crack gives a scalar moment tensor per unit volume of

$$m_s = \frac{9}{2}\frac{\lambda+2\mu}{\lambda+\mu}\frac{K_{Ic}}{(\pi a\cos\chi)^{1/2}}\frac{D_0}{\sin\chi\cos^2\chi}\left[\left(\frac{D}{D_0}\right)^{1/3}-1\right]^{1/2} \tag{6}$$

while tensile opening of the wing cracks give

$$m_t = \frac{3(\lambda+2\mu)^2}{2\mu(\lambda+\mu)}\frac{K_{Ic}}{(\pi a\cos\chi)^{1/2}}D_0\left[\left(\frac{D}{D_0}\right)^{1/3}-1\right]^{5/2} \tag{7}$$

A complete specification of the moment tensor for the damage requires that the orientation of the cracks be considered. We did this by transforming the local coordinates of the initial cracks (which varied with position around the source) to a fixed coordinate system for wave propagation to a specified field point. These transformations are straightforward but messy and are given in Johnson and Sammis (2001).

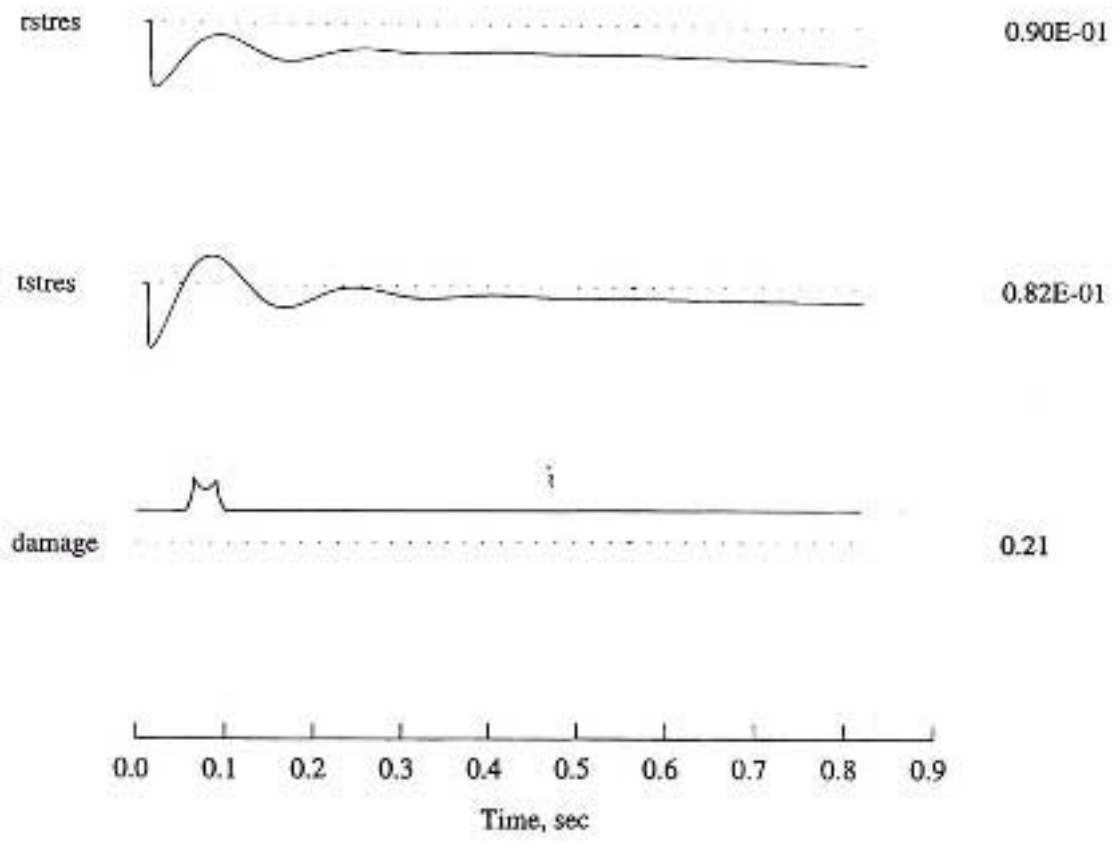

Figure 5. Calculated radial stress, tangential stress, and damage for a distance of 35 m from the NPE explosion. The numbers on the right are peak stress in units of GPa for the stresses. An initial damage of D_0=0.10 and an initial crack radius of a=0.10 cm were used in these calculations (from Johnson and Sammis, 2001).

The net contribution of the damage to the radiated signal is calculated as an integral over the entire damage zone, taking into account the amount of damage, the orientation of the cracks, and the time history of the motion on the cracks at each point in this zone. Such integrals were obtained by numerical methods using the following procedure:

- The region surrounding the source was divided into a large number of small volume elements.
- The equivalent elastic method was used to calculate the principal stresses within each volume element as a function of time.
- Equation (3) was used to determine if an increase in damage occurred within the volume element and, if so, the amount of increase ant the time at which it begins.
- The increase in damage was converted to a moment tensor.
- The displacements at the receiver location were calculated by using a Green function and integrating over every volume element where there was an increase in damage.
- The results of these calculations for the NPE explosion are summarized in Tables 1 and 2.

Table 1. Effect of Initial Damage

Initial Damage D_0	Failure Damage D_f	Failure radius r_f (m)	Damage radius r_d (m)	Maximum Velocity V_{max} (450 m), cm/sec
0.01	0.09	25	25	0.9
0.05	0.26	35	45	8.4
0.10	0.40	35	45	16.1
0.20	0.53	35	45	28.2
0.40	0.73	35	45	44.8
0.80	1.13	35	45	88.9

Crack radius a=0.1 cm in all cases

Table 2. Effect of Initial Crack Radius

Crack radius a	Failure Damage Df	Failure radius rf (m)	Damage radius rd (m)	Maximum Velocity Vmax (450 m) cm/sec
0.01	0.22	18	18	2.6
0.10	0.40	35	45	16.1
1.00	0.39	75	90	21.1
10.0	0.40	90	150	13.1

Initial damage D_0=0.1 in all cases.

Figure 6 shows the waveforms for a range of different initial crack sizes.

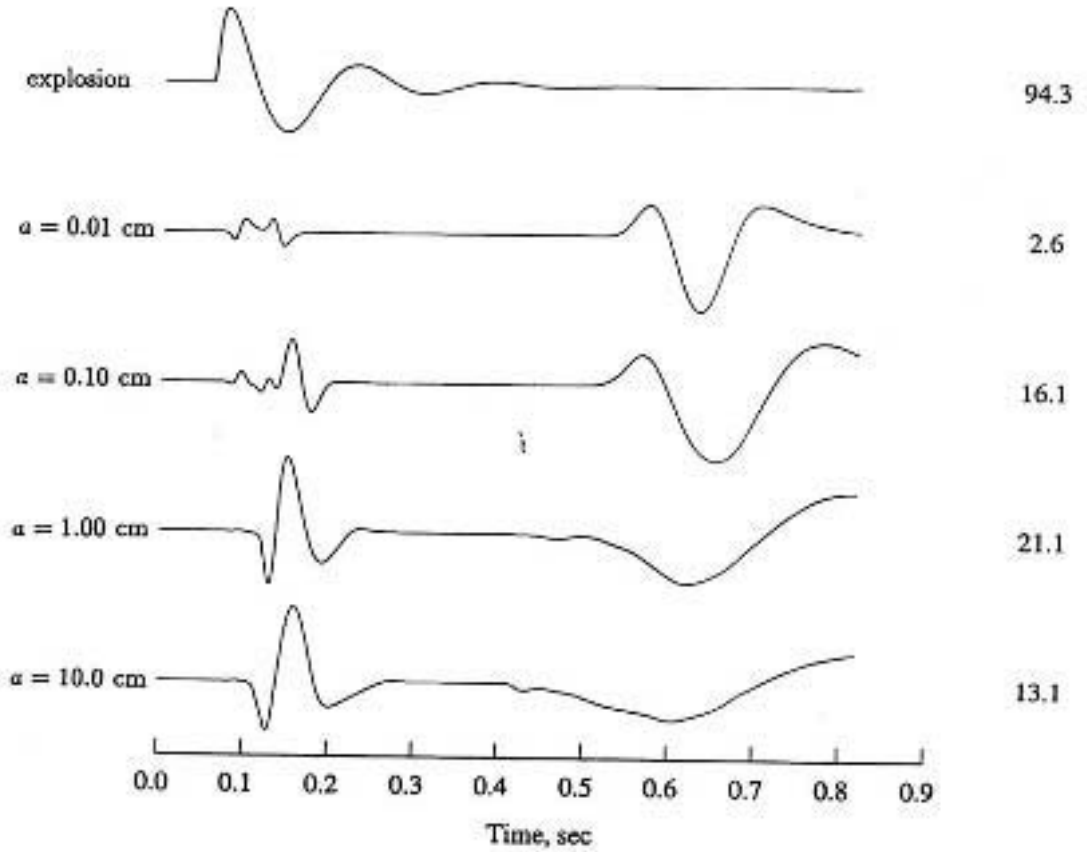

Figure 6. Effect of initial crack radius on the radiated secondary waves for an initial damage of D_0=0.10 (from Johnson and Sammis, 2001).

CONCLUSIONS AND RECOMMENDATIONS

This study has considered one of the processes that may occur in the region of high stresses immediately surrounding an explosion detonated in rock, the extension of pre-existing cracks. Using a combination of analytical and numerical methods, the physics of this crack extension process has been modeled. The results have interesting and significant implications with regard to the elastic waves that are radiated by explosive sources.

Combining the equivalent elastic method of calculating stresses in the near-source region of an explosion (Johnson, 1993) with a micro-mechanical damage model (Ashby and Sammis, 1990) leads to an approximate but efficient method of estimating the growth of pre-existing cracks. Sample calculations for the NPE chemical explosion revealed that the stress waves from the explosion were capable of generating significant amounts of crack growth in an extensive region surrounding the source, with the extent and shape of this region depending upon such parameters as the initial damage, the size of the cracks, the amount of pre-stress and orientation of the cracks. These calculations suggest that the extent of the damaged zone is most sensitive to the initial crack radius, varying from a radial distance of about 45 m for a crack radius of 0.1 cm to about 150 m for a crack radius of 10 cm for this 1 kt explosion. These numbers are consistent with the results reported by Rimer *et al*. (1998) for Russian explosions in hard rocks, which underwent intensive fracturing extending out to a scaled radius of 40 $m/kt^{1/3}$ and occasional fracturing observed out to about 200 $m/kt^{1/3}$.

These calculations also suggest that the growth of the cracks does not occur at the time of peak stress, but significantly later when the tangential stress is relaxing more rapidly than the radial stress. This leads to a damage front that follows behind the outward propagating stress wave with a velocity between those of P and S waves. In addition to calculating the time when the cracks begin to grow, it is also possible to calculate the amount of growth and the orientation of the cracks that are growing. This information is sufficient to calculate a seismic moment tensor for the crack growth, which in turn can be used to calculate the secondary elastic waves generated by the crack growth. Because two different processes accomplish crack growth, sliding on the pre-existing cracks and the extension of wing cracks, the moment tensor also consists of two different parts. Thus one of the contributions of this study is a procedure for estimating the secondary elastic waves that are generated when there is growth of cracks in a zone surrounding an explosion.

While the contribution from a single crack is small, the integration over the many cracks in a large zone of increased damage surrounding an explosion may lead to the generation of seismic waves that are comparable in amplitude to those of the explosion itself. For an isotropic homogeneous distribution of cracks, the composite moment tensor is isotropic and thus radiates only P waves into the far field. However, any departure from spherical symmetry in the problem leads to the generation of S waves. In this paper we investigated two types of asymmetry 1) a pre-stress in the vicinity of the explosion and 2) a preferred orientation of the cracks in the vicinity of the explosion. Both types of asymmetry have similar effects if the pre-stress and crack orientations are chosen in a consistent manner. Included in these effects are significant S waves that emerge from the region surrounding the explosion and thus appear to be generated by the explosion itself.

The effects of crack growth calculated in this paper should be regarded as minima because the increase in damage was stopped at the inception of failure. Damage is likely to continue beyond this point but we are not aware of a suitable method of calculating damage, along with stress and strain in the unstable post-failure regime. This is one aspect of the problem that definitely needs further research. Sammis (1998) has suggested acoustic fluidization (Melosh, 1979) as a possible method of modeling this type of behavior, and this aspect of the problem is currently being pursued.

Another area in which further research would be useful is a more complete connection between the equivalent elastic treatment and the damage mechanics. In the present study the shear modulus and energy loss are modeled using empirical relations borrowed from the soil mechanics. In principle, it should be possible to calculate the change in elastic moduli caused by a change in damage using a method such as that of O'Connell and Budiansky (1974) and to calculate the loss of energy due to the damage directly from fracture mechanics.

Finally, the method should be further tested against the recorded waveforms from the larger U.S. nuclear explosions in granite (Hardhat, Piledriver, and Shoal) and the Russian hard rock waveforms when they become available in digital form next year.

REFERENCES

Ashby, M.F., and C.G. Sammis (1990), The damage mechanics of brittle solids in compression, *PAGEOPH*, **133**, 489-521.

Denny, M. D., Introduction and highlights, in Proceedings of the Symposium on the Non-Proliferation Experiment (NPE): Results and Implications for Test Ban Treaties, M. D. Denny (editor), CONF-9404100, Department of Energy, 1994.

Glenn, L. A. (1993), Energy-density effects on seismic decoupling, *J. Geophys. Res*., **98**, 1933-1942.

Glenn, L. A., and P. Goldstein (1994), Seismic decoupling with chemical and nuclear explosions in salt, *J. Geophys. Res.*, **99**, 11,723-11,730.

Johnson, L. R., Wave propagation near explosive sources, PL-TR-93-2118, Phillips Laboratory, 22 pp., 1993.

Johnson, L.R. and C.G. Sammis (2001), Effects of rock damage on seismic waves generated by explosions, *Pure and Applied Geophysics*, **158**, 1869-1908.

King, D. S., B. E. Freeman, D. D. Eilers, and J. D. Johnson (1989), The effective yield of a nuclear explosion in a small cavity in geologic material: enhanced coupling revisited, *J. Geophys. Res*., **94**, 12,375-12,385.

Melosh, H. J. (1979), Acoustic fluidization: A new geologic process, *J. Geophys. Res*., **84**, 7513-7520.

O'Connell, R. J., and B. Budiansky (1974), Seismic velocities in dry and saturated cracked solids, *J. Geophys. Res*., **79**, 5412-5426.

Olsen, K. H., and A. L. Peratt, Free-field ground motion for the non-proliferation experiment: preliminary comparisons with nearby nuclear events, in Proceedings of the Symposium on the Non-Proliferation Experiment (NPE): Results and Implications for Test Ban Treaties, M. D. Denny (editor), CONF-9404100, Department of Energy, 1994.

Rimer, N., J. L. Stevens, J. R. Murphy, and G. G. Kocharyan, Estimating seismic characteristics of explosions in hard rock using a micro-mechanical damage model, p. 392-400 in Proceedings of the 20th Annual Seismic Research Symposium on Monitoring a Comprehensive Test Ban Treaty, J. Fantroy, D. Heatley, J. Warren, F. Chavez, and C. Meade (eds), Department of Defense and U.S. Department of Energy, 1998.

Rodean, H. C., Nuclear-Explosion Seismology, U. S. Atomic Energy Commission, TID-25572, 156 pp., 1971.

Sammis, C. G., Acoustic fluidization in the damage regime of explosions in crystalline rock, p. 417-421 in Proceedings of the 20th Annual Seismic Research Symposium on Monitoring a Comprehensive Test Ban Treaty, J. Fantroy, D. Heatley, J. Warren, F. Chavez, and C. Meade (eds), Department of Defense and U.S. Department of Energy, 1998.

Smith, C. W., NPE - close-in stress and motion measurements, in Proceedings of the Symposium on the Non-Proliferation Experiment (NPE): Results and Implications for Test Ban Treaties}, M. D. Denny (editor), CONF-9404100, Department of Energy, 1994.